

¹*G. Chandra Shekar
²P. Naveen Kumar

Estimation and Evaluation of Ionospheric Scintillations at Various NavIC Signal Frequencies using Real Time Data



Abstract: - The ionospheric scintillations affect radio waves from the NavIC satellites through the ionosphere. The ionospheric scintillations lower receiver tracking accuracy, integrity, and continuity. This paper presents the computation of ionosphere parameters such as TEC, ROTI and scintillation index (S) using pseudo range and Carrier to Noise density ratio (C/No) measurements of NavIC L5 and S-band signals. Also, investigates the ionospheric scintillations, which are common in the equatorial and low latitude region. The correlation between the amplitude scintillation index S4 and ROTI is investigated using real data of NavIC receiver at Osmania University, Hyderabad. The results obtained confirm that the scintillations impact varies with radio signal frequency and it is severe on low frequencies during post sunset hours at low latitude regions.

Keywords: NavIC; Scintillation; TEC; ROTI.

I. INTRODUCTION

Navigation with Indian Constellation (NavIC) is an indigenous satellite navigation system developed and deployed by the Indian Space Research Organization (ISRO) for position, navigation, and time (PNT) applications in a limited-service region. With three Geostationary Orbital Satellites (GEO) and four Geosynchronous Orbital Satellites (GSO), it is completely operational. Users in the Indian subcontinent can observe at least four satellites at any given moment thanks to the way the satellites were orbited. The NavIC satellites use a Binary Phase-Shift Keying (BPSK (1)) modulation on L5 (1176.45MHz) to transmit navigation signals based on Code Division Multiple Access (CDMA) for users of the standard positioning service (SPS). Restricted service customers receive signals modified with a Binary Offset Carrier (BOC(5,2)) on S-band (2492.028 MHz) [1]. For satellite-based communication and navigation systems, the ionosphere serves as a propagation medium. It has several impacts on signals, including refraction, absorption, scintillation, Faraday rotation, propagation time delay, and Doppler frequency shift. The ionospheric scintillations are abrupt temporal fluctuations in the amplitude and phase of trans-ionospheric Global Navigation Satellite System (GNSS) signals. There are more ionospheric scintillations, especially in high latitudes and equatorial regions. Moreover, the ionospheric scintillations pose a risk to a broad spectrum of radio frequencies, making them extremely useful in real-world scenarios. The significant research on ionospheric scintillations were published in [2-5]. Furthermore, the irregularities of the ionosphere were studied using signals from the Global Positioning System (GPS). Ionospheric scintillations were studied by Swamy et al. (2013) & Sarma et al. (2014), who created mathematical models to forecast ionospheric scintillations over the Indian region using GPS signals [6]–[7]. In order to investigate ionosphere irregularity, Pi et al. (1997) introduced the Rate of TEC Index (ROTI). Later, Basu et al. (1999) [8]–[9] examined the relationship between ROTI and S4-index (ROTI/S4). It is important to determine the intensity of those ionospheric scintillation events because a decrease in the number of GNSS satellites available will impact positioning accuracy when there is a synchronization issue between the satellite and the receiver. In a preliminary study on the amplitude scintillation effect of NavIC signals, Sujimol and Shahana (2017) discovered frequent lock loss on L5 signals at Delhi station [10]. In this paper we use NavIC data on L5 and S-band frequencies to compute ionosphere medium irregularity indicators such as S4 and ROTI. Moreover, a critical analysis is done with respect to elevation angle, time and frequency of signal.

II. NAVIC DATA ACQUISITION AND SCINTILLATIONS ESTIMATION

A receiver station located at the Department of ECE, UCE, OU, Hyderabad, India, recorded NavIC satellite signals at sampling rate of 1Hz, in order to analyse the abnormalities in the ionosphere. In receiver set up, a 15-meter low loss RF wire connects receiver unit with dual-band antenna which was installed on the roof of ECE

¹ *Corresponding author: Research Scholar, Department of ECE, College of Engineering, Osmania University, Hyderabad, India-500 007. Email: chandu.vnr2016@gmail.com

²Professor, Department of ECE, College of Engineering, Osmania University, Hyderabad, India, 500 007.

Copyright © JES 2024 on-line : journal.esrgroups.org

building. The binary data recorded in the receiver were extracted into a standard form using "IrnssUR" tool. After that TEC, ROTI, and S4-index were computed.

The S4 index and ROTI are the two different parameters used to analyse the ionosphere irregularities. In this work, S4-index is calculated using carrier to noise density ratio(C/N₀) [9], and ROTI is computed using TEC data/ionospheric delay. The ROTI can be used as the alternate of S4 index [10] to analyse ionosphere irregularities.

The ratio of the standard deviation to the mean value of the averaged C/N₀ is how the amplitude scintillation index S₄ is determined [9]. The scintillations can be categorized into 3 different levels, strong scintillations when S₄ is above 0.6, moderate scintillations when S₄ is between 0.3 and 0.6, and weak scintillations when S₄ is less than 0.3 are used to categorize the effectiveness of the amplitude scintillations index [11]. This is the calculation used to get the amplitude scintillations.

$$S_4 = \sqrt{\frac{\langle SI^2 \rangle - \langle SI \rangle^2}{\langle SI \rangle^2}} \tag{1}$$

Where, SI is the trans-ionospheric signal intensity as received

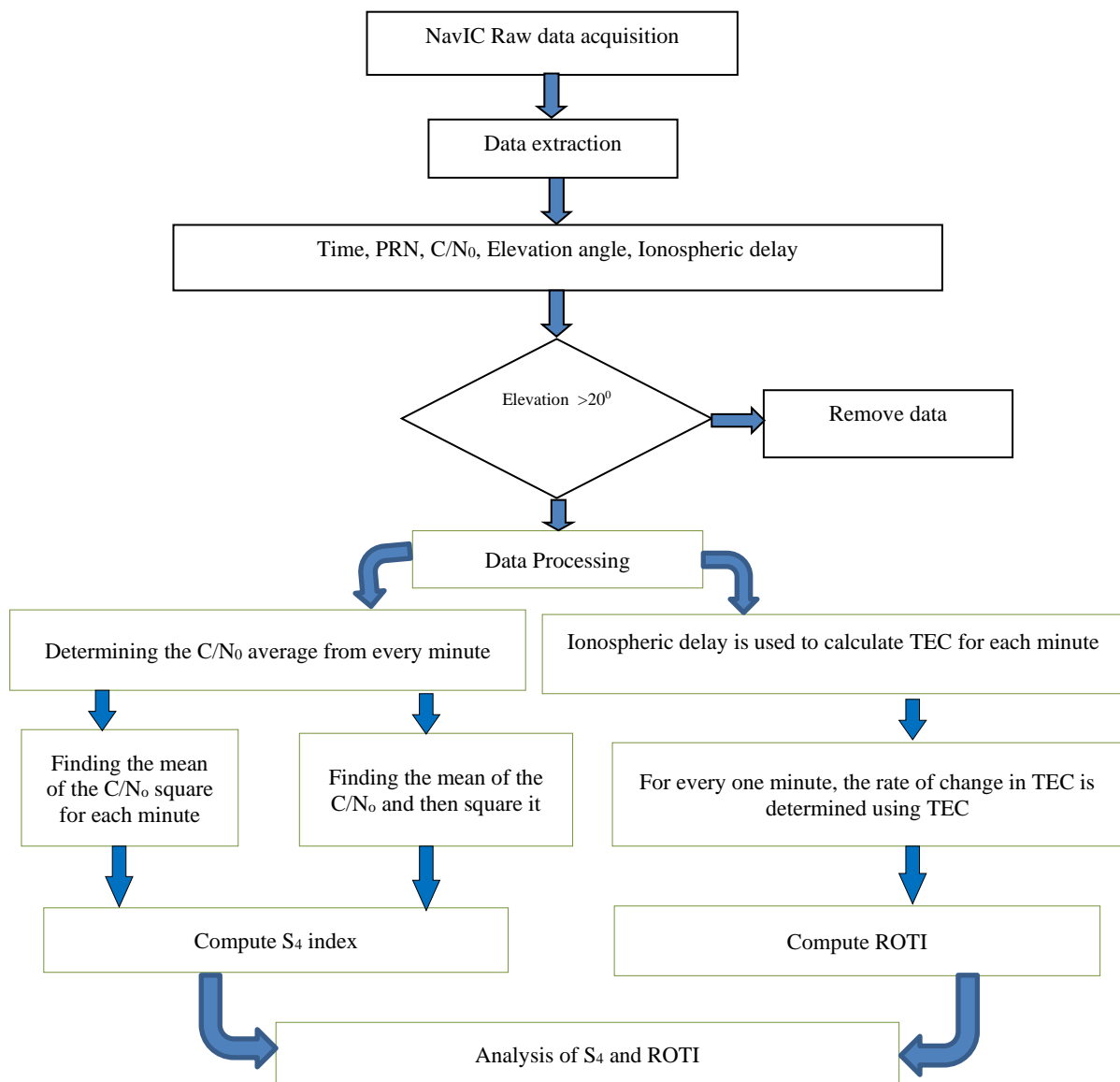


Fig.1. Methodology of proposed work

The S4 index defined in Eqn.(1) includes the ambient noise, it can be expressed in terms of carrier-to-noise density ratio (C/N0) as,

$$S4_{N0} = \sqrt{\frac{100}{C/N_0} \left[1 + \frac{500}{19C/N_0} \right]} \tag{2}$$

After removing the noise, the revised value of S4-index is

$$S4 = \sqrt{\frac{(SI^2) - (SI)^2}{(SI)^2} - \frac{100}{C/N_0} \left[1 + \frac{500}{19C/N_0} \right]} \tag{3}$$

The second approach calculates ROTI by utilizing the ionosphere-induced delay in the signals that are received [12]. From ionospheric delay (I_D) TEC data can be calculated using the expression given below:

$$TEC = I_D * f^2 / 40.3 \tag{4}$$

Where I_D is the ionospheric delay on the frequency (f) of the received trans-ionospheric signal and TEC is the Total Electron Content (TEC) of the ionosphere along the signal path. The TEC is measured in TECU and is expressed as follows:

$$1TECU = 10^{16} \text{ e/m}^2 \tag{5}$$

At regular intervals, the rate of change of TEC (ROT) is determined by (5):

$$ROT = \frac{TEC_b^a - TEC_{b-1}^a}{t_b - t_{b-1}} \tag{6}$$

Where a indicates a particular satellite and b the epoch time. The computation of ROTI is based on the ROT standard deviation.

$$ROTI = \sqrt{\langle ROT^2 \rangle - \langle ROT \rangle^2} \tag{7}$$

Three categories characterize the effectiveness of ROTI: Weak when the index falls between 0.25 and 0.5, modest when the index falls between 0.5 and 1, strong when it rises above 1 [13–14].

III. RESULTS AND DISCUSSION

The data of NavIC receiver, which were sampled at 1 Hz are considered for calculation and analysis of S4-index, and ROTI. Fig.2 shows S4-index of L5 and S-band signal and ROTI variation for I02 satellite on June 07, 2020. In Figure 2, C/No variation is also plotted along with S4-index and ROTI for I02 satellite. To analyse all the index parameter at bottom panel of the figure the elevation angle of the satellite is also presented. For this particular I02 satellite the elevation angle is varied between 300 – 700. From the figure we could observe that the scintillation event is occurred during post sun set around 15 Hrs (UTC) hrs (15+5:30= 20:30 Hrs (Local Time)).

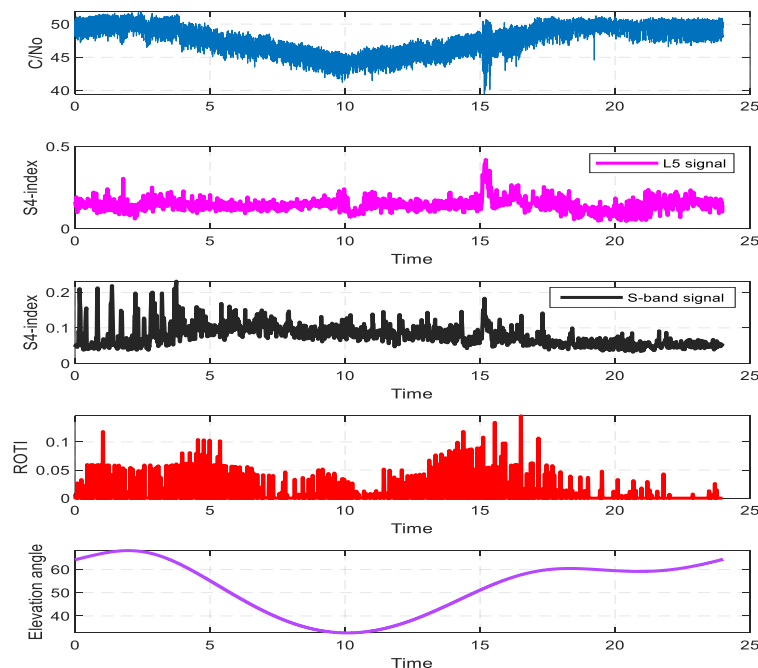


Fig.2. L5, S-band signal S4 and ROTI variation for I02 satellite of

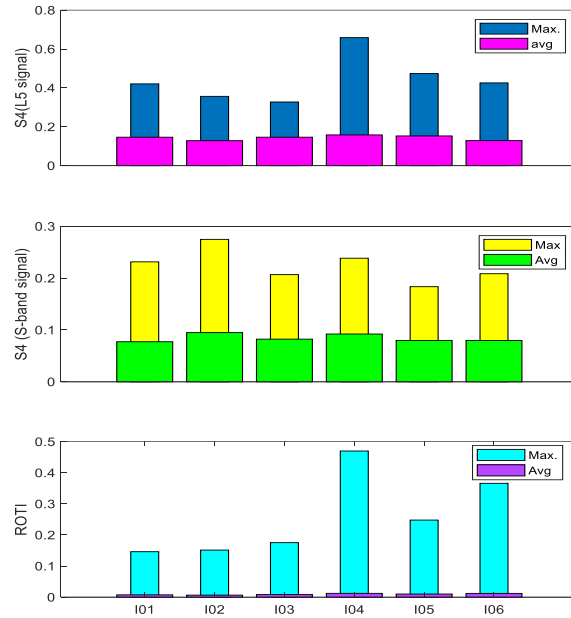


Fig.3. Statistics of S4-index (L5 and S-Band) and ROTI measured NavIC I02

At the time of scintillation event S4 index value for L5 and S-band signals is 0.41 and 0.22 respectively at the elevation of 54° and 56° . At that epoch ROTI is also high and it is 0.1 TECU/min. Also, observed that the scintillations impact is high on L5 signal compared to that of S-band signal of NavIC constellation. Like this the estimation and analysis of S4, and ROTI index is done for I03, I04, I05, I06 and I07 satellites of same constellation, the results obtained are analyzed statistically as shown in Fig.3.

From Fig.3, it is clear that S4-index measured on L5 frequency and ROTI are at their maximum for PRN I05 which is in Geosynchronous orbit. However, S4-index measure on S-band is maximum for I03 satellite from which the signal is received at low elevation angle.

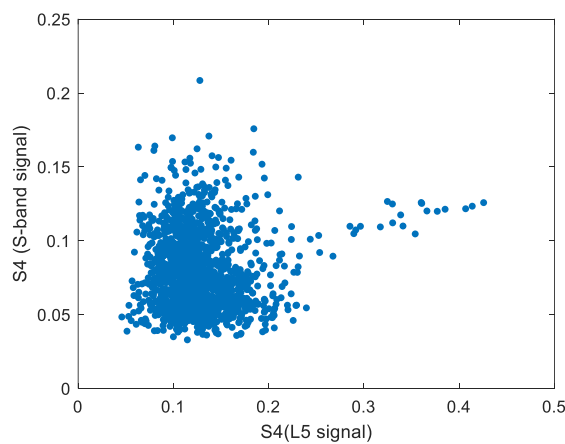


Fig.4. Relation of S4 (L5 signal) and S4 (S-Band signal) using I02 data

The statistics of S4-index and ROTI are depicted in Table 1. Both maximum and average values of S4-index are high for L5-signal. Moreover, ROTI maximum and mean values are high for I05. From these observations we

can clearly say that ROTI and S4-index measured on L5 are showing the same behavioral trend. Further, a clear investigation is also done to understand the relation between S4-index of L5 and S-band signals.

Fig. 4 shows the relation between S4-index of L5 and S-band signals. Almost all the S4-index values of S-band are in a bin of 0.05 and 0.2. Likewise, for L5 signal most of the S4-index values are between 0.05 and 0.2. a very few values are greater than 0.3 and 0.4.

Table.1. S4-index and ROTI statistics measured using L5 and S-band signals of NavIC

PRN	Max. of S4		Average of S4		Max. of ROTI	Average of ROTI
	L5	S-Band	L5	S-Band		
I02	0.42	0.23	0.14	0.07	0.14	0.007
I03	0.35	0.27	0.12	0.09	0.15	0.006
I04	0.32	0.20	0.14	0.08	0.17	0.008
I05	0.65	0.23	0.15	0.09	0.45	0.012
I06	0.47	0.18	0.15	0.07	0.24	0.010
I07	0.42	0.20	0.12	0.07	0.36	0.012

Frequency dependence of Scintillations

Fremouw et (1978) predicted the frequency dependence of ionospheric scintillations, and has given a mathematical model for it as [15],

$$S_4(f) = S_4(f_k) \left(\frac{f_k}{f}\right)^{1.5} \tag{8}$$

$S_4(f)$ is the S4-index to be predicted on the frequency ‘ f ’, $S_4(f_k)$ is the S4-index known on the frequency ‘ f_k ’. The model is applied to predict the S4-index of L1, L2 and S-band frequencies results depicted in Fig.5. To further study the relation, S4 of S-band measured is plotted against S4 of S-band predicted with respect to the measured.

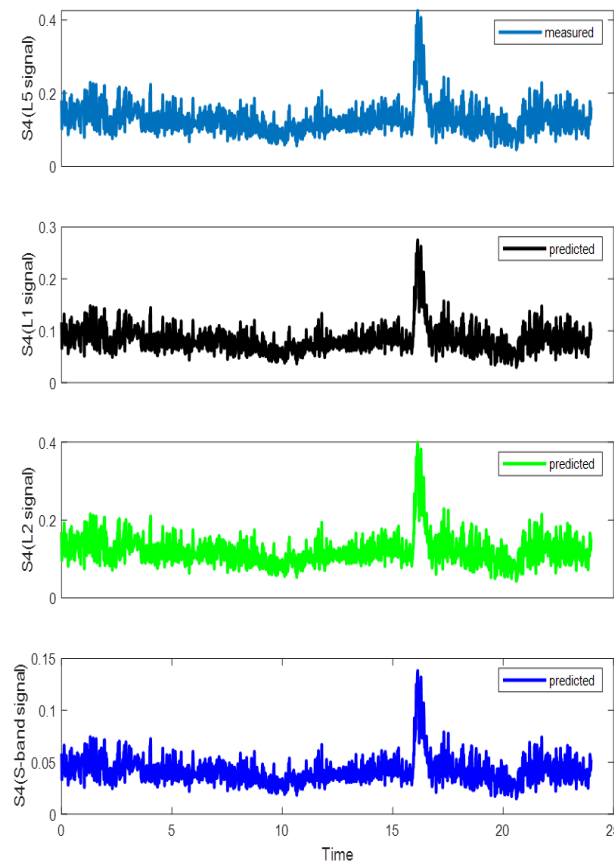


Fig. 5. Predicted S4 of GPS (L1 and L2) and NavIC S-band signals using NavIC L5 signal

In Fig.5, top panel shows S4-index measured on L5 frequency, bottom three panels show the predicted S4-index on L1, L2 and S-band frequencies respectively. The S4-index measured on L5 frequency, the maximum is 0.4. It is decreased to 0.26 and 0.135 for the frequency of L1 and S-band signals respectively. It states that the scintillations impact decreases as the frequency of radio signal increases.

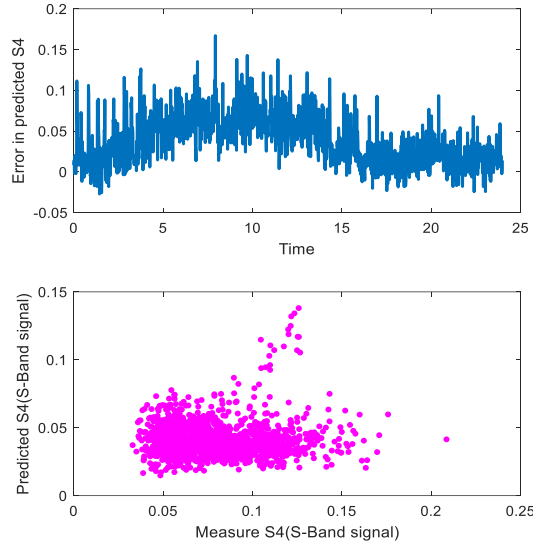


Fig.6 Relation between measured and predicted S4 of NavIC S-band signal

Fig. 6 shows measured S4 index of S-band and its range. In figure, top panel shows the error in predicted S4 with respect to the measured. Most of the times, the predicted S4 value is less than the measured. It can also be noticed that the model performance is good during post sun-set hours relative to the day time. Moreover, the model performance is not same for all the frequencies. Therefore, the model is needs to be modified according to the signal frequency.

Tracking jitter ($\sigma_{\phi,J}^2$)

When the receiver phase locked loop breaks to lock the arrival signal then the signal is said to have phase error which is called as tracking jitter. The value where PLL fails to lock is given as [16-17]

$$\sigma_{\phi_e/lim}^2 = \left[\frac{\pi}{12} \right]^2 \text{ rad}^2$$

Tracking jitter for amplitude scintillation and phase scintillation if there is no correlation then it is given as [18-20]

$$\sigma_{\phi,J}^2 = \sigma_{\phi_s}^2 + \sigma_{\phi_T}^2 + \sigma_{\phi_{osc}}^2$$

Where $\sigma_{\phi_s}^2$ = phase scintillation component

$\sigma_{\phi_T}^2$ = thermal noise component

$\sigma_{\phi_{osc}}^2$ =oscillator noise component

$\sigma_{\phi_{osc}}^2 = 0.1 \text{ rad}^2$ which is constant

Phase scintillation jitter is resolved as

$$\sigma_{\phi}^2 = 2 \int_{\tau}^{\infty} S_{\phi_p}(f) df$$

In this case, the receiver’s phase stability time is identified by the system parameter. the phase scintillation component is described as follows :

$$\sigma_{\theta_s}^2 = \frac{\pi T}{k f_n^{p-1} \sin\left(\frac{(2k+1-p)\pi}{2k}\right)} \quad \text{for } 1 < p < 2k$$

Where k =order of PLL
 f_n is loop natural frequency
 T = spectral strength

When the thermal noise component of amplitude scintillation increases and the received signal strength will be decreases, the result is given as:

$$\sigma_{\theta_T}^2 = \frac{B_n \left[1 + \frac{1}{2\eta (C/N_0) (1 - 2S_{4c}^2)} \right]}{(C/N_0) (1 - S_{4c}^2)}$$

Where B_n = bandwidth of PLL
 C/N_0 = carrier to noise ratio
 η = predetection integration time($1 < \eta < 20$ ms)
 S_4 = Amplitude scintillation in signal
 The above formula is valid for $S_4 < 0.707$.

In this paper, we use amplitude scintillation index and spectral parameters P and T for NavIC signals of all PRNs of L-band and S-band simultaneously to calculate tracking jitter.

From figure 7-12 it is clear that the S_4 and tracking jitter of L5 band gradually increases from 9:10am IST and are at peaks at 1:38pm IST and then decreases from 6:40pm IST. From figure 13-18, it is clear that the S_4 and tracking jitter of S band gradually increases from 9:30am IST and are at peaks at 10:50am IST and then decreases from 3:50pm IST (Indian standard time). Figure shows S_4 tracking jitter for all PRNs of L-band, the S_4 and tracking jitter values for all PRNs are tabulated in table 2.

By the table the S_4 values ranges from 0.0468 to 0.4235 and tracking jitter ranges from 0.5895 rad² to 0.6346 rad². The lowest S_4 , tracking jitter recorded were 0.0468 in PRN2 as shown in figure (7-12) on 1:30pm IST ,0.4794 rad² in PRN3 as shown in figure (7-12) on 9:23am IST respectively and the highest were 0.4235 in PRN3 as shown in figure (7-12) on 1:38pm IST,0.6346 rad² in PRN3 on 1:38pm IST as shown in figure (7-12) respectively. Figure 2 shows S_4 tracking jitter for all PRNs of S-band, the S_4 and tracking jitter values for all PRNs are tabulated in table 3. By the table the S_4 values ranges from 0.027 to 0.2793 and tracking jitter ranges from 0.4602 rad² to 0.6197 rad². The lowest S_4 , tracking jitter recorded were 0.0278 in PRN4 as shown in figure (13-18) on 11:02pm IST ,0.4602 rad² in PRN3 on 1:08am IST as shown in figure (13-18) respectively and the highest were 0.2793 in PRN3 as in fig (13-18-),0.6197 rad² in PRN2 as shown in figure (13-18) respectively.

Table.2. Scintillation Values for L-band

PRN	L-BAND					
	Amplitude Scintillation (S_4)			Tracking Jitter ($\sigma_{\theta,J}^2$) (rad ²)		
	MIN	MAX	MEAN	MIN	MAX	MEAN
2	0.0468	0.3217	0.151	0.4878	0.5895	0.519
3	0.05607	0.4235	0.1514	0.4794	0.6346	0.504
4	0.05473	0.3555	0.1554	0.4974	0.5987	0.5298
5	0.06821	0.3092	0.1507	0.4973	0.6194	0.5373
6	0.06222	0.3075	0.1558	0.5123	0.5979	0.5448
7	0.06476	0.2959	0.1384	0.5164	0.6063	0.544

Table.3. Scintillation Values for S-band

PRN	S-BAND					
	Amplitude Scintillation (S_4)			Tracking Jitter ($\sigma_{\theta,J}^2$) (rad ²)		
	MIN	MAX	MEAN	MIN	MAX	MEAN
2	0.03077	0.2424	0.07761	0.4762	0.6197	0.5292
3	0.03032	0.2793	0.0973	0.4602	0.5599	0.4862

4	0.02785	0.2118	0.08334	0.4722	0.5893	0.5093
5	0.03624	0.2511	0.09461	0.4749	0.5681	0.5182
6	0.03168	0.1868	0.08136	0.522	0.5916	0.5497
7	0.03276	0.2116	0.08089	0.5076	0.5788	0.5292

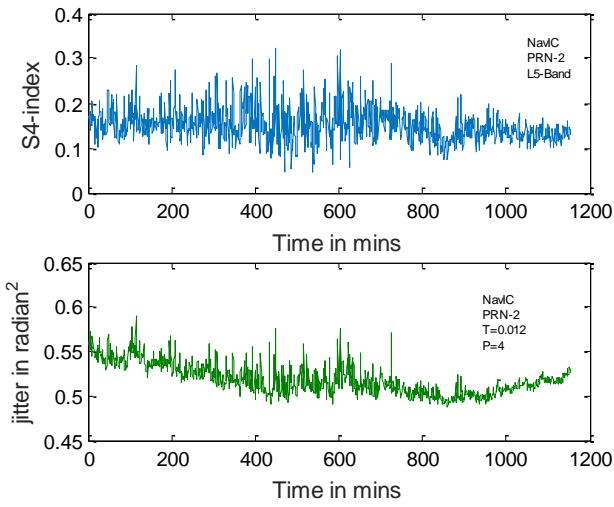


Fig.7. NavIC PRN-2

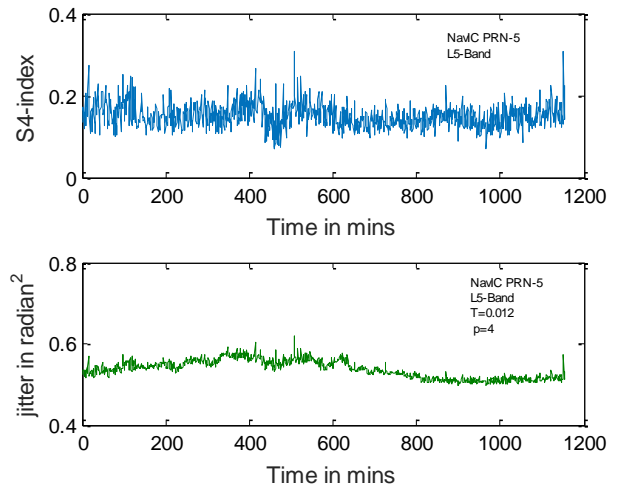


Fig.10. NavIC PRN-5

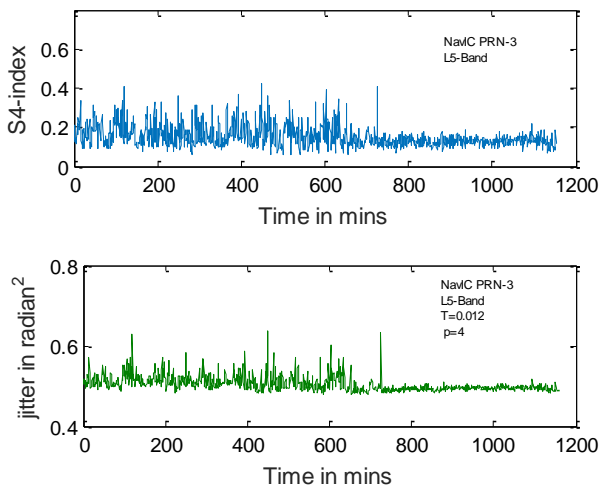


Fig.8. NavIC PRN-3

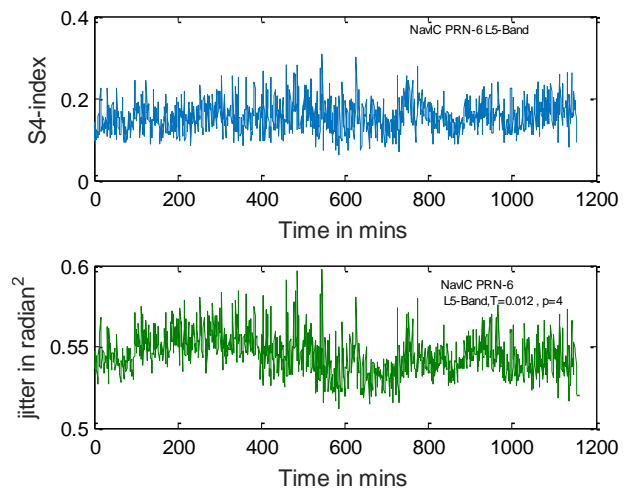


Fig.11. NavIC PRN-6

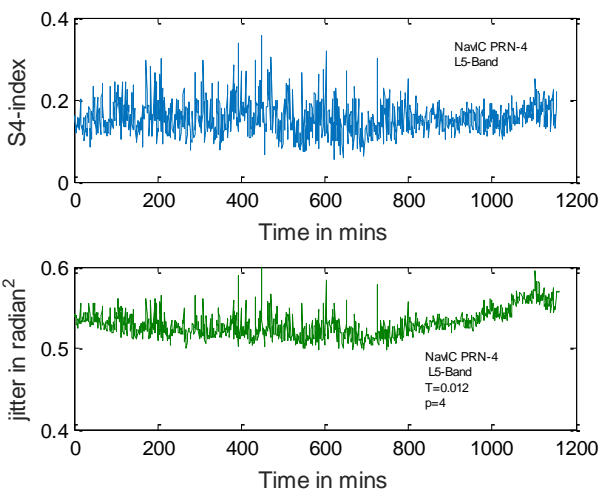


Fig.9. NavIC PRN-4

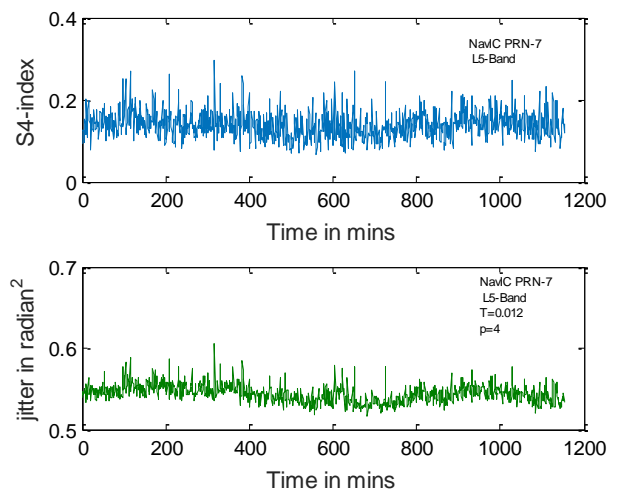


Fig.12. NavIC PRN-7

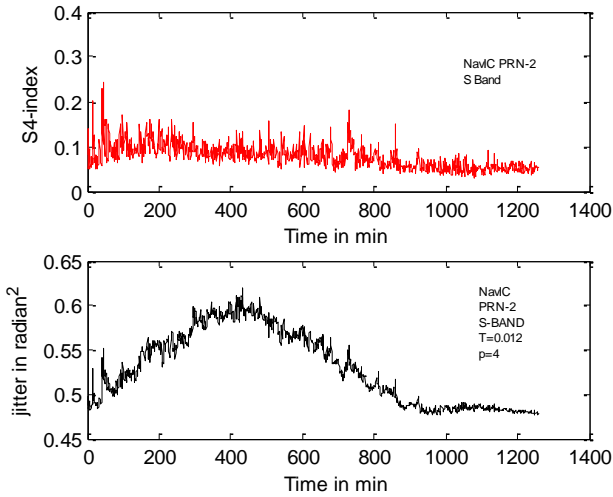


Fig.13. NavIC PRN-2

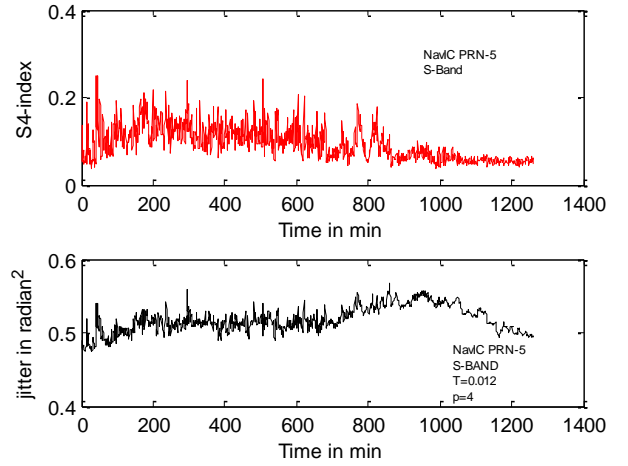


Fig.16. NavIC PRN-5

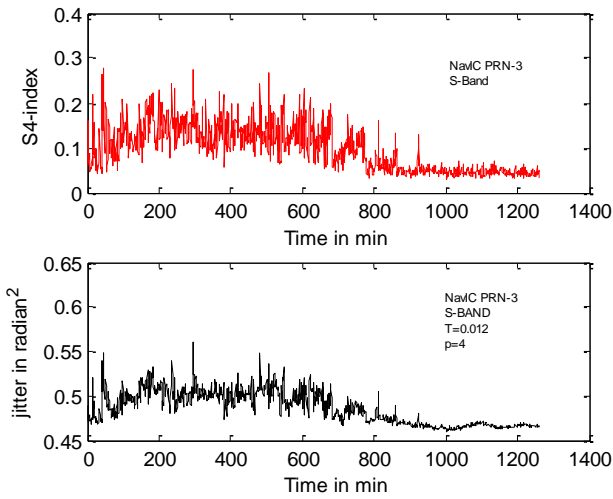


Fig.14. NavIC PRN-3

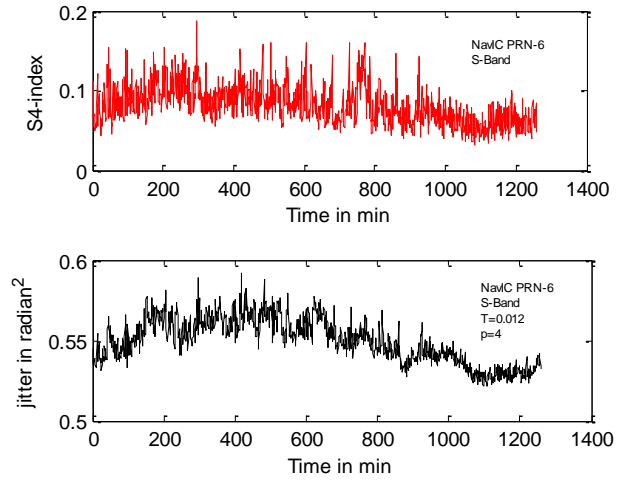


Fig.17. NavIC PRN-6

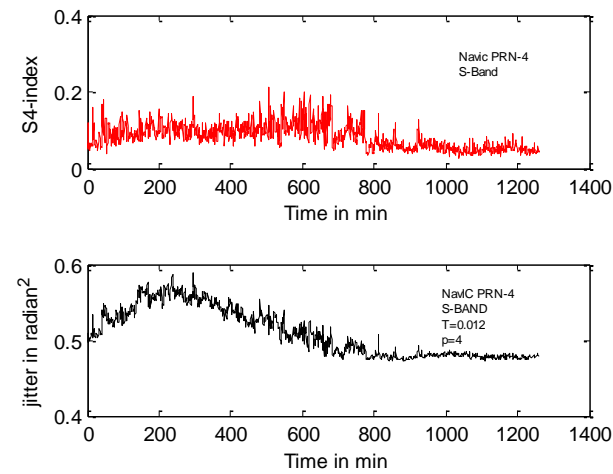


Fig.15. NavIC PRN-4

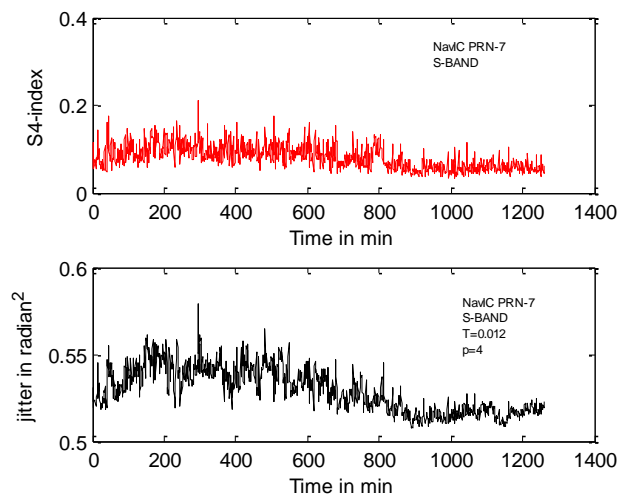


Fig.18. NavIC PRN-7

IV. CONCLUSION

This article presented the analysis of NavIC trans-ionospheric signals for a typical date 08-09-2017. In order to identify the ionospheric perturbations, the amplitude of the scintillation index S4, the rate of the change of total electron content index (ROTI) are computed on L5 and S-band frequencies of NavIC constellation. Further, this article presented a step-by-step procedure for S4 -index measurement without ambient noise effect. Based on the correlative analysis, maximum similarity between the S4 index and ROTI is observed, and, thus ROTI can be considered as an alternative index for the investigation of the amplitude scintillations. It is also observed that the ionospheric scintillations are robust only on L5 frequency. Additionally, we have found that low frequency (L5) signals are extremely sensitive to ionosphere variations, and that the influence of ionosphere changes is greater on low elevation GEO satellite communications.

REFERENCES

- [1] Indian Space Research Organisation (ISRO). Indian Regional Navigation Satellite System: Signal in Space ICD for Standard Positioning Service, Version 1.0; ISRO Satellite Centre: Bengaluru, India, 2014.W.-K. Chen, Linear Networks and Systems (Book style). Belmont, CA: Wadsworth, 1993, pp. 123–135.
- [2] Aarons J, Global morphology of ionospheric scintillation, Proc IEEE (USA), 70(4) 360, 1982.
- [3] Aarons J, The longitudinal morphology of equatorial F-layer irregularities relevant to their occurrence, Space Sci Rev (USA), 63, 209 , 1993.
- [4] Basu S & Basu S, Equatorial scintillations: Advances since ISEA-6, J Atmos Terr Phys (UK), 47, 753, 1985.
- [5] Basu S & Basu S, Remote sensing of auroral E region plasma structures by radio, radar, and UV techniques at solar minimum, Journal of Geophysical Research Atmospheres, 98(A2):1589-1602,1993.
- [6] K.C.T. Swamy, A. D Sarma & A. Supraja Reddy, V. Satya Srinivas, P.V.D. Somasekhar Rao, Modelling of GPS signal scintillations with polynomial coefficients over the Indian region, Indian Journal of Radio & Space Physics (IJRSP) IJRSP, vol. 42, no. 3, 2013.
- [7] AD Sarma, K.C.T. Swamy & PVD Somasekhar Rao, Forecasting of ionospheric scintillations of GPS L-band signals over an Indian low latitude station, 2014 IEEE Antennas and Propagation Society International Symposium (APSURSI), 265-266, 2014.
- [8] Pi X, Manucci A J, Lindqwister U J & Ho C M, Monitoring of global ionospheric irregularities using worldwide GPS network, Geophys Res Lett (USA), 24, 2283, 1997.
- [9] Sunanda Basu & Ceasar Valladares, Global aspects of plasma structures, Journal of Atmospheric and solar –Terrestrial Physics 61, 127-139, 1999.
- [10] M R Sujimol & K Shahana, Ionospheric scintillation characteristics in IRNSSL5 and S- band signals, Indian Journal of Radio & Space Physics ,Vol 45, March 2017 ,pp 15-19, 2018.
- [11] Wernik A.W, Alfonsi L & Materassi M, Scintillation modeling using in situ data, 36 Radio Sci. 42, 1–21. doi:10.1029/2006RS003512, 2007.
- [12] Swapna Raghunath & D Venkata Ratnam, Detection of ionospheric spatial and temporal gradients for ground based augmentation system applications, Indian Journal of Radio & Space Physics, Vol 45, March 2016, pp 11-19, 2016.
- [13] Swamy K.C.T, Sarma A.D, Satya Srinivas V, Accuracy evaluation of estimated ionospheric delay of GPS signals based on Klobuchar and IRI-2007 models in low latitude region, IEEE Geosci. Remote Sens, Lett.,10, (6), pp. 1557–1561 (doi: 10.1109/LGRS.2013.2262035), 2013.
- [14] Smita Dubei, Rashmi Wahi, Ekkaphon Mingkhan & A K Gwal, Study of amplitude and phase scintillation at GPS frequency, Indian Journal of Radio & Space Physics, Vol. 34, pp. 402-407, 2005.
- [15] Fremouw, W. J., & Zitter, R. E. (1978). A comparison of skills training and cognitive restructuring–relaxation for the treatment of speech anxiety. Behavior Therapy, 9(2), 248–259.
- [16] Conker, R. S., M. B. El - Arini, C. J. Hegarty, and T. Hsiao, Modeling the effects of ionospheric scintillation on GPS/Satellite - Based Augmentation System availability, Radio Sci., 38(1), 1001, doi:10.1029/ 2000RS002604, 2003
- [17] Swamy, K.C.T. Global navigation satellite system and augmentation. Resonance, 22, 1155–1174 . <https://doi.org/10.1007/s12045-017-0579-6>, 2017.
- [18] Feng, J.; Liu, D.; Zhen, W. The study of ionospheric scintillation model with satellite signal. Glob. Position Syst., 38, 13–15. (In Chinese), 2013.
- [19] K.C.T. Swamy, D. Venkata Ratnam and Towseef Ahmed Shaik, "Double difference method with zero and short base length carrier phase measurements for Navigation with Indian Constellation satellites L5 (1176.45 MHz) signal quality analysis", *Int. J. Satell. Commun. Networking*, vol. 40, no. 4, pp. 294-304, 2022.
- [20] K.C.T. Swamy, A.D. Sarma, AS Reddy and TK Pant, "Analysis of ionospheric scintillations of GPS and VHF/UHF signals over low latitude Indian region", World Congress on Information and Communication Technologies, pp. 400-403, 2012.